

***Ab initio* calculation of the linewidth of various phonon modes in germanium and silicon**

G. Deinzer, G. Birner, and D. Strauch

Institut für Theoretische Physik, Universität Regensburg, D-93040 Regensburg, Germany

(Received 27 April 2002; revised manuscript received 30 October 2002; published 28 April 2003)

The $2n+1$ theorem and the density-functional perturbation theory have been used to calculate anharmonic force constants completely *ab initio*. Explicit expressions for the anharmonic coupling constants are presented, i.e., for the third-order derivatives of the total energy with respect to atomic displacements. Using the harmonic as well as the anharmonic results the phonon linewidth of Ge and Si as a function of temperature has been calculated for various branches and various (in particular, for nonvanishing) wave vectors completely *ab initio*.

DOI: 10.1103/PhysRevB.67.144304

PACS number(s): 63.20.Kr, 63.20.Ry, 31.15.Ar, 71.15.Mb

I. INTRODUCTION

Harmonic-phonon properties of the covalent semiconductors are nowadays quite well understood due to a large number of experimental data and due to various calculations. Density-functional perturbation theory (DFPT) has been applied successfully to the *ab initio* determination of linear-response lattice properties of these materials such as phonon frequencies and eigenvectors.^{1,2} But within this approach no anharmonic contribution to the lattice oscillations are included. However, one is also interested in more subtle physical quantities which are due to the anharmonicity of the lattice potential such as the temperature dependence of lifetimes and frequency shifts of phonon modes. But these quantities are of extreme importance in modern technology and are leading to a deeper understanding of the interplay between electronic and dynamical properties.

Numerical model results have been obtained some 40 years ago.³ First *ab initio* results have been obtained by frozen-phonon methods;⁴ but only Γ -point features are accessible with this method without the use of supercells, and the numerical expense of supercell calculation for other points in the Brillouin zone is enormous.

The extension of density-functional theory (DFT) to non-linear response functions with the help of the $2n+1$ theorem⁵ has established the possibility to calculate the non-linear expansion coefficients of the total energy from first-order wave functions. Within this approach a selected set of anharmonic force constants⁶ and nonlinear susceptibilities^{7,8} has been evaluated from first principles. In recent work also the Raman tensor of various semiconductor compounds has been calculated directly.⁹ The realistic results of these calculations have encouraged us to investigate still different non-linear coefficients.

Recent developments of inelastic neutron-scattering instrumentation are aimed at measuring the linewidth of phonon modes other than at the Γ point and bring theoretical calculation thereof into focus.¹⁰ In addition, the thermal conductivity, which is a very essential quantity in modern semiconductor technology, is closely related to the linewidth. All the ingredients necessary for calculating this quantity can be obtained by the theory below.

To the best of our knowledge, the application of DFPT methods to the anharmonic force constants has been restricted so far to the special case of the LO and TO phonons

at the Γ point. Within this approach the linewidth and frequency shift of these modes of the elemental semiconductors,^{6,11} III-V compounds,^{12,13} and 3C-SiC¹⁴ have been computed.

In this work, we extend and apply an *ab initio* method to the calculation of linewidth of arbitrary modes in germanium and silicon. To this end, the Taylor coefficients of the total energy are calculated via DFPT. Within the framework of interacting-phonon theory these are used to determine the linewidth.

An alternative approach to compute the linewidth and frequency as a function of temperature has been performed by Wang *et al.*¹⁵ who have used molecular-dynamics simulations with a semiempirical tight-binding ansatz for the energy. To determine the tight-binding Hamiltonian, they have used only first-principles data obtained from band-structure and total-energy calculations. This method has the advantage of including the anharmonicity to arbitrary order; but it is restricted to high temperatures, as it treats the atomic motion classically, and it must fail in the low-temperature regime, where quantum effects are important.

II. EXPANSION OF THE ENERGY

The Hamiltonian of a crystal can be written in terms of creation operators $a^\dagger(\lambda)$ and annihilation operators $a(\lambda)$ of phonons with quantum number λ , harmonic frequencies ω_λ , and phonon field operators $A(\lambda) = a(\lambda) + a^\dagger(\bar{\lambda})$,

$$H = \hbar \sum_{\lambda} \omega_{\lambda} [a^\dagger(\lambda)a(\lambda) + \frac{1}{2}] + H_A. \quad (1)$$

We use the notation $\lambda = (\mathbf{q}, j)$ and $\bar{\lambda} = (-\mathbf{q}, j)$ with wave vector \mathbf{q} and branch index j . The first part of Eq. (1) describes the energy resulting from harmonic oscillators with energies $\hbar \omega_\lambda$. The anharmonic Hamiltonian H_A can be written up to an arbitrary order n in terms of either phonon field operators $A(\lambda)$ or atomic displacements $u_\alpha^\kappa(\mathbf{R})$ in the direction α of an atom κ in the unit cell determined by the lattice vector \mathbf{R} as

$$\begin{aligned}
H_A &= \sum_{n \geq 3} \frac{1}{n!} \sum_{\mathbf{R}_1, \dots, \mathbf{R}_n} \sum_{\alpha_1, \dots, \alpha_n} \Phi_{\alpha_1, \dots, \alpha_n}^{\kappa_1, \dots, \kappa_n}(\mathbf{R}_1, \dots, \mathbf{R}_n) \\
&\quad \times u_{\alpha_1}^{\kappa_1}(\mathbf{R}_1) \cdots u_{\alpha_n}^{\kappa_n}(\mathbf{R}_n) \\
&= \sum_{n \geq 3} \frac{\hbar}{n!} \sum_{\lambda_1, \dots, \lambda_n} V_n(\lambda_1, \dots, \lambda_n) A(\lambda_1) \cdots A(\lambda_n).
\end{aligned} \tag{2}$$

The expansion coefficients $\Phi_{\alpha_1, \dots, \alpha_n}^{\kappa_1, \dots, \kappa_n}(\mathbf{R}_1, \dots, \mathbf{R}_n)$ are the derivatives of the total energy E with respect to the atomic displacements

$$\Phi_{\alpha_1, \dots, \alpha_n}^{\kappa_1, \dots, \kappa_n}(\mathbf{R}_1, \dots, \mathbf{R}_n) = \frac{\partial^n E}{\partial u_{\alpha_1}^{\kappa_1}(\mathbf{R}_1) \cdots \partial u_{\alpha_n}^{\kappa_n}(\mathbf{R}_n)}. \tag{3}$$

With the expansion of the displacements $u_{\alpha}^{\kappa}(\mathbf{R})$,

$$u_{\alpha}^{\kappa}(\mathbf{R}) = \sum_{\lambda} \sqrt{\frac{\hbar}{2NM_{\kappa}\omega(\lambda)}} e_{\alpha}^{\kappa}(\lambda) e^{i\mathbf{q} \cdot \mathbf{R}} A(\lambda) \tag{4}$$

in terms of phonon field operators $A(\lambda)$, the transformation of the coefficients in Eq. (7) is given by

$$\begin{aligned}
V_3(\lambda_1, \lambda_2, \lambda_3) &= \left(\frac{\hbar}{8N^3 \omega(\lambda_1) \omega(\lambda_2) \omega(\lambda_3)} \right)^{1/2} \\
&\quad \times \sum_{\substack{\kappa_1 \kappa_2 \kappa_3 \\ \alpha_1 \alpha_2 \alpha_3}} \Psi_{\alpha_1 \alpha_2 \alpha_3}^{\kappa_1 \kappa_2 \kappa_3}(\mathbf{q}_1, \mathbf{q}_2, \mathbf{q}_3) \\
&\quad \times \frac{e_{\alpha_1}^{\kappa_1}(\lambda_1)}{\sqrt{M_{\kappa_1}}} \frac{e_{\alpha_2}^{\kappa_2}(\lambda_2)}{\sqrt{M_{\kappa_2}}} \frac{e_{\alpha_3}^{\kappa_3}(\lambda_3)}{\sqrt{M_{\kappa_3}}} \\
&\quad \times e^{i\mathbf{q}_1 \cdot \mathbf{R}_1} e^{i\mathbf{q}_2 \cdot \mathbf{R}_2} e^{i\mathbf{q}_3 \cdot \mathbf{R}_3},
\end{aligned} \tag{5}$$

with eigenvector $e_{\alpha}^{\kappa}(\lambda)$ and the mass M_{κ} of the atom κ .

In the following, we will consider just the third-order term. The contributions of the fourth- and higher-order terms will be neglected. In the framework of DFPT^{5,16} one transforms the atomic displacements into the reciprocal space via

$$\mathbf{u}^{\kappa}(\mathbf{q}) = \frac{1}{\sqrt{N}} \sum_{\mathbf{R}} e^{-i\mathbf{q} \cdot \mathbf{R}} \mathbf{u}^{\kappa}(\mathbf{R}). \tag{6}$$

and evaluates directly the Fourier transforms of the third-order anharmonic force constants

$$\begin{aligned}
\Psi_{\alpha_1 \alpha_2 \alpha_3}^{\kappa_1 \kappa_2 \kappa_3}(\mathbf{q}_1, \mathbf{q}_2, \mathbf{q}_3) &= \delta_{\mathbf{q}_1 + \mathbf{q}_2 + \mathbf{q}_3, \mathbf{G}} \sum_{\mathbf{R}_1, \mathbf{R}_2, \mathbf{R}_3} \Phi_{\alpha_1 \alpha_2 \alpha_3}^{\kappa_1 \kappa_2 \kappa_3}(\mathbf{R}_1, \mathbf{R}_2, \mathbf{R}_3) \\
&\quad \times e^{i\mathbf{q}_1 \cdot \mathbf{R}_1} e^{i\mathbf{q}_2 \cdot \mathbf{R}_2} e^{i\mathbf{q}_3 \cdot \mathbf{R}_3}.
\end{aligned} \tag{7}$$

The Kronecker δ symbol expresses the conservation of the crystal quasimomentum. (This follows from the translational invariance of the crystal.) Until now the quantity Ψ on the left-hand side of equation Eq. (7) has only been evaluated for the special case $\mathbf{q}_1 = 0$, $\mathbf{q}_2 = -\mathbf{q}_3$.

From the $2n+1$ theorem the knowledge of both the Kohn-Sham Hamiltonian and the Kohn-Sham wave functions up to first order is sufficient to determine the third-order response function.⁵

III. THIRD-ORDER DENSITY-FUNCTIONAL PERTURBATION THEORY

In the Born-Oppenheimer approximation, one separates the ionic and electronic contributions. The calculation of the ionic contribution is performed via Ewald-summation techniques.¹⁷ The explicit expressions can be found in Ref. 12. The electronic contribution is calculated in DFPT in the following way.

The first-order perturbation expansion of the Kohn-Sham equation

$$H_{\text{KS}}|\psi_{\alpha}\rangle = \varepsilon_{\alpha}|\psi_{\alpha}\rangle, \tag{8}$$

results in the so-called Sternheimer equation,

$$\left(\frac{\partial H_{\text{KS}}}{\partial \lambda} - \varepsilon_{\alpha}^{(1)} \right) |\psi_{\alpha}\rangle = (H_{\text{KS}} - \varepsilon_{\alpha}) \left| \frac{\partial \psi_{\alpha}}{\partial \lambda} \right\rangle. \tag{9}$$

All the needed quantities (Hamiltonians and wave functions) can be calculated either self-consistently or via minimization of the energies.¹⁸

The explicit calculation of the anharmonic coefficients is preferably carried out in reciprocal space analogous to Eq. (7). Then the reciprocal-space anharmonic constants of Eq. (7) are given as the third-order derivatives of the total energy E_{tot} with respect to the displacements of Eq. (6),

$$\Psi_{\alpha_1 \alpha_2 \alpha_3}^{\kappa_1 \kappa_2 \kappa_3}(\mathbf{q}_1, \mathbf{q}_2, \mathbf{q}_3) = \frac{\partial^3 E_{\text{tot}}}{\partial u_{\alpha_1}^{\kappa_1}(\mathbf{q}_1) \partial u_{\alpha_2}^{\kappa_2}(\mathbf{q}_2) \partial u_{\alpha_3}^{\kappa_3}(\mathbf{q}_3)}. \tag{10}$$

The analytic expression of the electronic part of the anharmonic force constants is derived from the original $2n+1$ theorem.⁵ Since the coefficients $\Psi_{\alpha_1 \alpha_2 \alpha_3}^{\kappa_1 \kappa_2 \kappa_3}(\mathbf{q}_1, \mathbf{q}_2, \mathbf{q}_3)$ are symmetrical in the three ($i=1,2,3$) sets of $(\kappa_i, \alpha_i, \mathbf{q}_i)$ they are given by

$$\begin{aligned}
\Psi_{\alpha_1 \alpha_2 \alpha_3}^{\kappa_1 \kappa_2 \kappa_3}(\mathbf{q}_1, \mathbf{q}_2, \mathbf{q}_3) &= \tilde{\Psi}_{\alpha_1 \alpha_2 \alpha_3}^{\kappa_1 \kappa_2 \kappa_3}(\mathbf{q}_1, \mathbf{q}_2, \mathbf{q}_3) + \tilde{\Psi}_{\alpha_2 \alpha_3 \alpha_1}^{\kappa_2 \kappa_3 \kappa_1}(\mathbf{q}_2, \mathbf{q}_3, \mathbf{q}_1) \\
&\quad + \tilde{\Psi}_{\alpha_3 \alpha_1 \alpha_2}^{\kappa_3 \kappa_1 \kappa_2}(\mathbf{q}_3, \mathbf{q}_1, \mathbf{q}_2) + \tilde{\Psi}_{\alpha_1 \alpha_2 \alpha_3}^{\kappa_1 \kappa_3 \kappa_2}(\mathbf{q}_1, \mathbf{q}_3, \mathbf{q}_2) \\
&\quad + \tilde{\Psi}_{\alpha_3 \alpha_2 \alpha_1}^{\kappa_3 \kappa_2 \kappa_1}(\mathbf{q}_3, \mathbf{q}_2, \mathbf{q}_1) + \tilde{\Psi}_{\alpha_2 \alpha_1 \alpha_3}^{\kappa_2 \kappa_1 \kappa_3}(\mathbf{q}_2, \mathbf{q}_1, \mathbf{q}_3).
\end{aligned} \tag{11}$$

Every term can be evaluated in DFPT by inserting the projector \mathcal{P}_c onto the unperturbed conduction states¹⁶ and by using explicitly the time-inversion symmetry of the Bloch orbitals $\psi_{\mathbf{v}\mathbf{k}}(\mathbf{r})$ one obtains

$$\begin{aligned}
\tilde{\Psi}_{\alpha_1\alpha_2\alpha_3}^{\kappa_1\kappa_2\kappa_3}(\mathbf{q}_1, \mathbf{q}_2, \mathbf{q}_3) = & \frac{1}{3} \delta_{\mathbf{q}_1+\mathbf{q}_2+\mathbf{q}_3, \mathbf{G}} \delta_{\kappa_1\kappa_2} \delta_{\kappa_1\kappa_2} \sum_{\mathbf{v}\mathbf{k}} \left\langle \psi_{\mathbf{v}\mathbf{k}} \left| \frac{\partial^3 v_{\text{ext}}}{\partial u_{\alpha_1}^{\kappa_1}(0) \partial u_{\alpha_2}^{\kappa_2}(0) \partial u_{\alpha_3}^{\kappa_3}(0)} \right| \psi_{\mathbf{v}\mathbf{k}} \right\rangle \\
& + 2 \delta_{\kappa_1\kappa_2} \sum_{\mathbf{v}\mathbf{k}} \left\langle \psi_{\mathbf{v}\mathbf{k}} \left| \frac{\partial^2 v_{\text{ext}}}{\partial u_{\alpha_2}^{\kappa_2}(-\mathbf{q}_1) \partial u_{\alpha_3}^{\kappa_3}(0)} \mathcal{P}_c \left| \frac{\partial \psi_{\mathbf{v}\mathbf{k}}}{\partial u_{\alpha_1}^{\kappa_1}(\mathbf{q}_1)} \right. \right\rangle \\
& + 2 \sum_{\mathbf{v}\mathbf{k}} \left\langle \frac{\partial \psi_{\mathbf{v}\mathbf{k}}}{\partial u_{\alpha_1}^{\kappa_1}(-\mathbf{q}_1)} \left| \mathcal{P}_c \frac{\partial v_{\text{KS}}}{\partial u_{\alpha_2}^{\kappa_2}(\mathbf{q}_2)} \mathcal{P}_c \left| \frac{\partial \psi_{\mathbf{v}\mathbf{k}}}{\partial u_{\alpha_3}^{\kappa_3}(-\mathbf{q}_3)} \right. \right\rangle \\
& - 2 \sum_{\mathbf{v}\mathbf{v}'\mathbf{k}} \left\langle \frac{\partial \psi_{\mathbf{v}\mathbf{k}}}{\partial u_{\alpha_1}^{\kappa_1}(-\mathbf{q}_1)} \left| \mathcal{P}_c \left| \frac{\partial \psi_{\mathbf{v}'\mathbf{k}+\mathbf{q}_3}}{\partial u_{\alpha_2}^{\kappa_2}(-\mathbf{q}_2)} \right. \right\rangle \left\langle \psi_{\mathbf{v}\mathbf{k}+\mathbf{q}_3} \left| \frac{\partial v_{\text{KS}}}{\partial u_{\alpha_3}^{\kappa_3}(\mathbf{q}_3)} \right| \psi_{\mathbf{v}\mathbf{k}} \right\rangle \\
& + \frac{1}{6} \int d^3r d^3r' d^3r'' f_{\text{xc}}^{\text{LDA}}(\mathbf{r}, \mathbf{r}', \mathbf{r}'') \frac{\partial n(\mathbf{r})}{\partial u_{\alpha_1}^{\kappa_1}(\mathbf{q}_1)} \frac{\partial n(\mathbf{r}')}{\partial u_{\alpha_2}^{\kappa_2}(\mathbf{q}_2)} \frac{\partial n(\mathbf{r}'')}{\partial u_{\alpha_3}^{\kappa_3}(\mathbf{q}_3)}. \quad (12)
\end{aligned}$$

In the last line,

$$\begin{aligned}
f_{\text{xc}}^{\text{LDA}}(\mathbf{r}, \mathbf{r}', \mathbf{r}'') &= \frac{\partial^3 E_{\text{xc}}[n^{(0)}]}{\partial n(\mathbf{r}) \partial n(\mathbf{r}') \partial n(\mathbf{r}'')} \\
&= \delta(\mathbf{r}-\mathbf{r}') \delta(\mathbf{r}-\mathbf{r}'') \frac{\partial^3 E_{\text{xc}}[n^{(0)}]}{\partial n(\mathbf{r}) \partial n(\mathbf{r}') \partial n(\mathbf{r}'')}
\end{aligned}$$

is the third-order exchange and correlation functional which becomes local in the local-density approximation (LDA). For the numerical evaluation of Eq. (12), we have expanded the wave functions in a plane-wave basis set. One also recognizes in this equation that only the second- and third-order derivatives of the external potential v_{ext} is needed, whereas the Kohn-Sham potential $v_{\text{KS}} = v_{\text{ext}} + v_{\text{Hxc}}$ has to be determined only up to first order (v_{Hxc} is the sum of Hartree, exchange, and correlation potentials).

IV. THE LINEWIDTH

In the framework of the interacting-phonon theory^{3,19} the phonon propagator is given by

$$\frac{2\omega_\lambda}{\omega_\lambda^2 - \omega^2 + 2\omega_\lambda \Sigma_\lambda(\omega)}, \quad (13)$$

with the complex self-energy

$$\Sigma_\lambda(\omega) = \Delta_\lambda(\omega) - i\Gamma_\lambda(\omega). \quad (14)$$

The damping function $\Gamma_\lambda(\omega)$ is the negative of the imaginary part of the self-energy $\Sigma_\lambda(\omega)$. To lowest order in \hbar only the third-order term contributes to $\Gamma_\lambda(\omega)$, i.e., only three-phonon processes are considered. The damping function for a phonon mode with quantum number $\lambda = (\mathbf{q}, j)$ and $\bar{\lambda} = (-\mathbf{q}, j)$ is then given by

$$\begin{aligned}
\Gamma_\lambda(\omega) &= \frac{\pi}{2} \sum_{\mathbf{q}_1, j_1, j_2} |V_3(\bar{\lambda}, \lambda_1, \lambda_2)|^2 \\
&\times [(1 + n_{\lambda_1} + n_{\lambda_2}) \delta(\omega_{\lambda_1} + \omega_{\lambda_2} - \omega) \\
&+ 2(n_{\lambda_2} - n_{\lambda_1}) \delta(\omega_{\lambda_1} - \omega_{\lambda_2} - \omega)], \quad (15)
\end{aligned}$$

where $n_\lambda = (e^{\hbar\omega_\lambda/kT} - 1)^{-1}$ is the Bose-Einstein occupation number. Due to the crystal-quasimomentum conservation one has $\lambda_2 = (\mathbf{q}_2, j_2)$ with $\mathbf{q}_2 = -\mathbf{q} - \mathbf{q}_1 + \mathbf{G}$. With the coefficients of Eqs. (5), (11), and (12) one can evaluate the frequency-dependent damping function $\Gamma_\lambda(\omega)$.

The first term in square brackets in Eq. (15) describes the decay of a phonon (λ) into two phonons (λ_1 and λ_2) with lower frequencies (or vice versa), the so-called summation process; the second term describes the phonon up conversion where the phonon (λ) combines with a phonon (λ_2) to create a phonon (λ_1) with higher energy (or vice versa), the so-called difference process.

In a weakly anharmonic crystal, one has $\Gamma_\lambda(\omega) \ll \omega_\lambda$ for $\omega \approx \omega_\lambda$, and line-shape effects are not important; and thus the shape of a line is well approximated by a Lorentzian with a full width at half maximum (FWHM) being equal to $2\Gamma_\lambda(\omega_\lambda)$.

V. COMPUTATIONAL TECHNIQUES

The damping function (15) is related to the two-phonon density of states (TDOS)

$$D_{\mathbf{q}}^{(2)}(\omega) = \frac{1}{N} \sum_{\mathbf{q}', j, j'} \delta(\omega_{\mathbf{q}'j'} + \omega_{\mathbf{q}-\mathbf{q}'j} - \omega), \quad (16)$$

and weighted by the anharmonic force constants given by Eq. (5).

The reciprocal-space summation (integration) of the TDOS has been performed with the tetrahedron method^{20,21} on a very dense mesh of \mathbf{q} vectors with $\approx 1.5 \times 10^4$ \mathbf{q} points in the entire Brillouin zone (BZ). Standard DFPT techniques have been used to obtain the frequencies and eigenvectors at

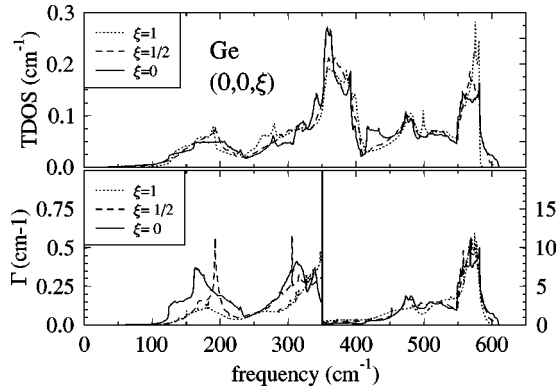


FIG. 1. Two-phonon density of states (upper panel) and damping function $\Gamma_{\mathbf{q},\text{LO}}$ of the LO mode (lower panel) of Ge at different points $(0,0,\xi)(2\pi/a)$ along the Δ direction at zero temperature. The harmonic frequencies are at 305.6, 293.8, and 242.8 cm^{-1} for $\xi=0, 0.5$, and 1. Note the change of scale in the lower panel.

these points in the harmonic approximation. We have used an $8 \times 8 \times 8$ Monkhorst-Pack²² mesh for the electronic states. The energy cut-off was set to 24 Ry. The pseudopotentials have been constructed following the standard method suggested by von Barth and Car.²³ We have decided to choose these potentials, because these potentials lead to excellent results for the phonon dispersion curves.¹ To describe the exchange and correlation energy, we have used the local-density approximation, as calculated by Monte Carlo techniques by Ceperley and Alder²⁴ with the interpolation proposed by Perdew and Zunger.²⁵

We have evaluated the Fourier transforms of the anharmonic force constants of Eqs. (7), (11), and (12) in DFPT as described in the preceding section. In contrast to previous work, we do not restrict ourselves to $\mathbf{q}=0$. The main difficulty arises in handling three different phonon wave vectors instead of two (\mathbf{q}_1 and $\mathbf{q}_2 = -\mathbf{q}_1$). From the computational point of view, the evaluation of Eq. (12) is not as expensive as the minimization procedures, which leads to the first-order wave functions.

The anharmonic force constants of Eq. (12) have been evaluated directly for a set of \mathbf{q}_1 and \mathbf{q}_2 vectors (with \mathbf{q}_3

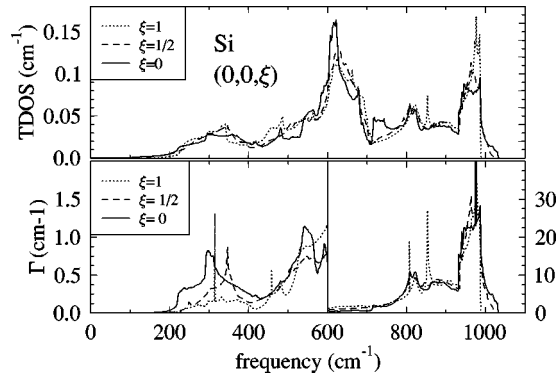


FIG. 2. Two-phonon density of states (upper panel) and damping functions $\Gamma_{\mathbf{q},\text{LO}}(\omega)$ of the LO mode (lower panel) of Si at different points $(0,0,\xi)(2\pi/a)$ along the Δ direction at zero temperature. The harmonic frequencies are at 517.0, 496.9, and 414.1 cm^{-1} for $\xi=0, 0.5$, and 1, respectively.

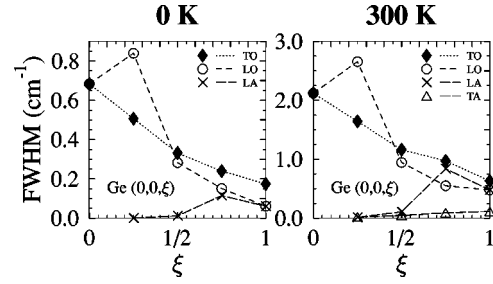


FIG. 3. The FWHM of the different modes along the Δ direction for germanium at zero temperature and 300 K. The lines are guides to the eye.

$= \mathbf{q}_1 + \mathbf{q}_2 + \mathbf{G}$) on a $4 \times 4 \times 4$ mesh. By taking advantage of the symmetry of the crystal the anharmonic force-constant tensors for 42 different $(\mathbf{q}_1, \mathbf{q}_2)$ pairs have to be calculated. The real-space coefficients of Eq. (3) are determined by Fourier transformation, and from the latter the reciprocal-space tensor elements of Eq. (7) are calculated on the dense mesh of around 1.5×10^4 \mathbf{q} vectors as ingredients for Eq. (15).

VI. RESULTS

We have first evaluated the TDOS at different \mathbf{q} points along the Δ direction. The results for Ge and Si are shown in Figs. 1 and 2, respectively. This calculation is purely harmonic.

Then we have calculated the damping function $\Gamma_{\lambda}(\omega)$ for the same \mathbf{q} points along the Δ direction. These quantities are also shown in Figs. 1 and 2, respectively. The difference in intensities between the TDOS and the damping function $\Gamma_{\lambda}(\omega)$ for a given \mathbf{q} is due to the anharmonic coupling parameters, while the fine structure of $\Gamma_{\lambda}(\omega)$ is determined by the TDOS. In the relevant one-phonon regime the damping functions are weak and show a smooth behavior, which justifies the assumption of a Lorentzian line shape with a FWHM given by $2\Gamma_{\lambda}(\omega_{\lambda})$.

The width $2\Gamma_{\lambda}(\omega_{\lambda})$ at the temperatures of 0 K and 300 K are displayed in Fig. 3 for Ge and in Fig. 4 for Si. The variation with \mathbf{q} is different for the different modes: The width of the TO mode decreases with increasing $|\mathbf{q}|$, whereas the one of the LO mode in Si first increases and then decreases faster than that of the TO mode. The LA-mode width increases up to the point $\mathbf{q} \approx \frac{3}{4}(0,0,1)(2\pi/a)$, and then decreases towards the zone-boundary X point [$\mathbf{q}=(0,0,1) \times (2\pi/a)$]. At zero temperature the FWHM for the TA mode

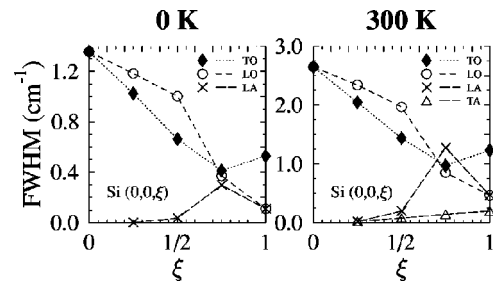


FIG. 4. Same as Fig. 3 but for Si.

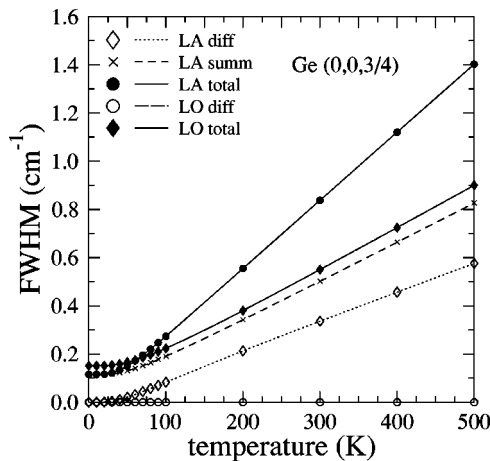


FIG. 5. Temperature dependence of the FWHM of the LO and LA mode in Ge at $\mathbf{q} = (0,0,3/4)(2\pi/a)$.

vanishes for kinematical reasons; at higher temperatures there is a slight increase, due to the difference processes (with always zero width at the Γ point).

At $\mathbf{q} = \frac{3}{4}(0,0,1)(2\pi/a)$ one can see the interesting fact that the LA-mode linewidth increases with temperature more than that of the other modes. Its FWHM is even greater than the one of the LO mode in both crystals, with the value being largest in Si. This behavior is due to the difference processes. No such processes have been found to contribute to the LO mode. For the LA and LO modes this feature is displayed for germanium in Fig. 5. Figure 6 shows the same for silicon.

Due to the experimental interest¹⁰ in the FWHM of low-frequency, dispersionless modes, we have investigated the TA branch in germanium in more detail. We have calculated the FWHM as a function of temperature at $\mathbf{q} = (0,0,\xi) \times (2\pi/a)$, with $\xi = 1/4$, $\xi = 1/2$, $\xi = 3/4$, as well as at the X point ($\xi = 1$). The results are displayed in Fig. 7. No summation processes contribute here due to the curvature of the lowest-frequency dispersion sheet. As demonstrated in Eq. (15) the first nonvanishing contribution in the summation-process term starts at the TA frequency.

In particular, in the low-temperature range quantum ef-

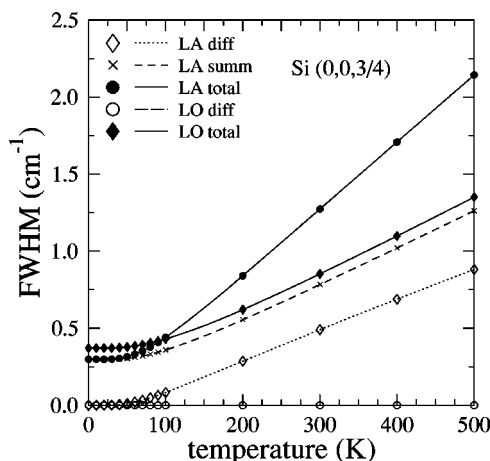


FIG. 6. Same as Fig. 5 but for Si.

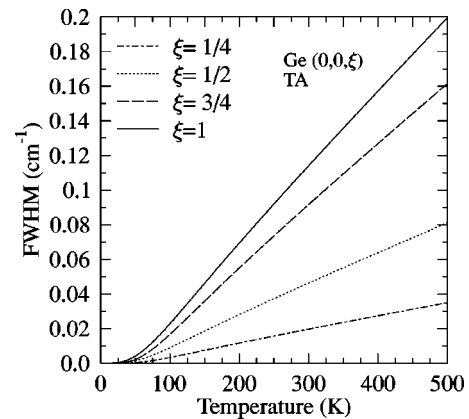


FIG. 7. Temperature dependence of the FWHM of the TA mode in Ge at different points $(0,0,\xi)(2\pi/a)$ along the Δ direction.

fects are important. However, even though there are contributions to $\Gamma_\lambda(\omega)$ even at $T = 0$ K, there are no decay channels for the TA modes; thus, their linewidth vanishes at zero temperature. In the higher-temperature range, we get a linear relation due to the Bose-Einstein occupation numbers. Beyond this range also higher-order terms may not be negligible. They will have to be investigated elsewhere.

First attempts¹⁰ to measure the TA-mode linewidth have shown that the resolution of the instrument is larger than the calculated linewidth.

Another approach to calculate the FWHM at the X point was performed by Wang *et al.*¹⁵ In contrast to the present work, they have used molecular-dynamics simulations with a semiempirical tight-binding Hamiltonian. Within this approach they are restricted to high temperatures. Supercells are needed to evaluate the FWHM at the X point. To the best of our knowledge no molecular-dynamics calculations are performed within the formalism of DFT. The values of Wang are higher than ours by up to a factor of 5. This may result from the higher-order anharmonic contributions, which are not included in our calculation. Another reason may be the use of a different Hamiltonian and the enormous (expensive) complexity of molecular-dynamics calculations. To make a comparative study, molecular-dynamics calculation based on a DFT Hamiltonian seem to be needed.

For Si, we have additionally calculated the FWHM along the Λ direction. The results are shown in Fig. 8 for Si at 0 K and 300 K. The results are qualitatively and quantitatively similar to those for the Δ direction except that the TO width

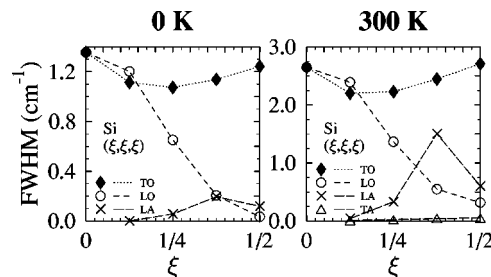


FIG. 8. The FWHM of different modes along the Λ direction for Si at 0 K and 300 K. The lines are guides to the eye.

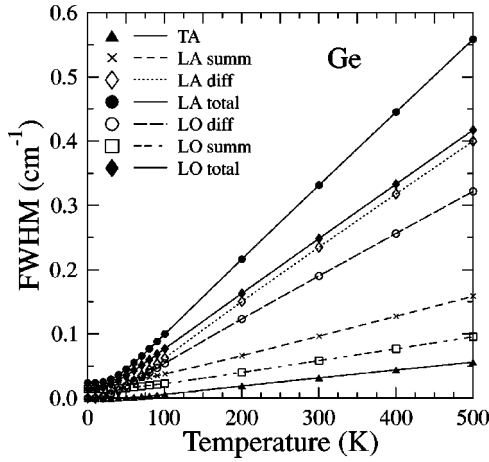


FIG. 9. Temperature dependence of the FWHM of the different modes in Ge at the L point.

is essentially independent of ξ , in contrast to that in the Δ direction.

The linewidth for a larger temperature range just for the L point for germanium is shown in Fig. 9 for the TA, LA, LO, and TO modes. The difference processes become the dominant part even at temperatures as low as 50 K. This is in contrast to the results for the Δ direction, where the summa-

tion processes always contribute at least as much as the difference processes.

VII. CONCLUSIONS

With the help of the $2n+1$ theorem, the anharmonic force constants can be calculated for arbitrary $(\mathbf{q}_1, \mathbf{q}_2)$ pairs in nonlinear DFPT. With the help of these quantities and within interacting-phonon theory, the linewidth of various phonon modes can be determined completely *ab initio*.

The coupling coefficients and the linewidth of various modes in Si and Ge have been evaluated, while previous calculations had been restricted to those at the Γ point.

Within the temperature domain considered ($0 \text{ K} \leq T \leq 300 \text{ K}$) the damping function is sufficiently small such that the linewidth is approximated by $2\Gamma_\lambda(\omega_\lambda)$ well enough. The present results show that the contributions from the summation and difference processes to the linewidth are very different for different branches at different \mathbf{q} points in different directions and that even qualitative predictions without reliable calculations seem impossible. The results present a challenge to the INS instrumentation under present development.

ACKNOWLEDGMENTS

We would like to thank the Deutsche Forschungsgemeinschaft (Contract No. STR 118/24) for the financial support of this work.

- ¹P. Giannozzi, S. de Gironcoli, P. Pavone, and S. Baroni, Phys. Rev. B **43**, 7231 (1991).
- ²S. Baroni, S. de Gironcoli, A. Dal Corso, and P. Giannozzi, Rev. Mod. Phys. **73**, 515 (2001).
- ³see, e.g., A.A. Maradudin, A.E. Fein, and G.H. Vineyard, Phys. Scr. **2**, 1479 (1962).
- ⁴S. Narasimhan and D. Vanderbilt, Phys. Rev. B **43**, 4541 (1991).
- ⁵X. Gonze and J.P. Vigneron, Phys. Rev. B **39**, 13 120 (1989).
- ⁶A. Debernardi, S. Baroni, and E. Molinari, Phys. Rev. Lett. **75**, 1819 (1995).
- ⁷A. Dal Corso and F. Mauri, Phys. Rev. B **50**, 5756 (1994).
- ⁸A. Dal Corso, F. Mauri, and A. Rubio, Phys. Rev. B **53**, 15 638 (1996).
- ⁹G. Deinzer and D. Strauch, Phys. Rev. B **66**, 100301 (2002).
- ¹⁰F. Demmel, R. Gähler, and J. Kulda (private communication).
- ¹¹G. Lang, K. Karch, M. Schmitt, P. Pavone, A.P. Mayer, R.K. Wehner, and D. Strauch, Phys. Rev. B **59**, 6182 (1999).
- ¹²A. Debernardi, Phys. Rev. B **57**, 12 847 (1998).
- ¹³A. Debernardi, Solid State Commun. **113**, 1 (2000).

- ¹⁴A. Debernardi, C. Ulrich, K. Syassen, and M. Cardona, Phys. Rev. B **59**, 6774 (1999).
- ¹⁵C.Z. Wang, C.T. Chan, and K.M. Ho, Phys. Rev. B **42**, 11 276 (1990); **40**, 3390 (1989).
- ¹⁶A. Debernardi and S. Baroni, Solid State Commun. **91**, 813 (1994).
- ¹⁷M. Born and K. Huang, *Dynamical Theory of Crystal Lattices* (Oxford University Press, Oxford, 1954).
- ¹⁸X. Gonze, Phys. Rev. A **52**, 1096 (1995).
- ¹⁹see, e.g., H. Bilz, D. Strauch, and R.K. Wehner, in *Handbuch der Physik, Bd. XXV/2d: Licht und Materie*, edited by S. Flügge (Springer, Berlin, 1984).
- ²⁰G. Lehmann and M. Taut, Phys. Status Solidi B **54**, 469 (1972).
- ²¹G. Gilat and N.R. Bharatiya, Phys. Rev. B **12**, 3479 (1975).
- ²²H.J. Monkhorst and J.D. Pack, Phys. Rev. B **13**, 5188 (1976).
- ²³U. von Barth and R. Car (unpublished).
- ²⁴D.M. Ceperley and B.J. Alder, Phys. Rev. Lett. **45**, 566 (1980).
- ²⁵J.P. Perdew and A. Zunger, Phys. Rev. B **23**, 5048 (1981).